



<sup>1</sup>. Erika VARGA-SIMON, <sup>2</sup>. Mária ÖRVÖS

## INFLUENCE OF HIDRODINAMIC FORCE AT CONVECTIV DRYING

<sup>1</sup>. Technical Institute, Faculty of Engineering, University of Szeged, Moszkvai bld. 5-7., Szeged, HUNGARY

<sup>2</sup>. Technical Institute, Faculty of Mechanical Engineering, Department of Building Service Engineering and Process Engineering, Budapest University of Technology and Economics, Bertalan Lajos str. 4-6., Budapest, HUNGARY

**Abstract:** The heat and mass transfer was studied in case of convective drying. The model spheres were made in different sizes from gypsum and the mixtures of gypsum and paper. The model spheres were taken into a drying chamber. The weight loss, the water content and the temperature of the product were tested on different air velocities during each experiment. The physical properties of the samples were measured in the interest of determination of heat transfer data. The calculated heat transfer coefficients on the basis of measured data have shown a difference from the results of heat transfer data – including dimensionless equations – derived from literature. The divergence at the heat transfer based on theoretically calculations and on practical measuring is deducible using the heat-, mass- and momentum balance. Our calculation supports a special hydrodynamic phenomenon with which the divergence is explained.

**Keywords:** heat and mass transfer, convective drying, model spheres, hydrodynamic phenomenon

### 1. INTRODUCTION

The removal of moisture from a food product is one of the oldest methods of preservation. When the water content of a food product is reduced to a very low level, the opportunity for microbial deterioration is minimized and the rates of other deteriorative reactions are reduced significantly. In addition to preservation, dehydration significantly reduces the product mass and volume and improves the efficiency of product transportation and storage.

To achieve the desired results for dehydrated foods, the optimum heat and mass transfer must be provided within the product, design of which necessitates careful analysis of the processes of heat and mass transfer.

Drying involves removal of the moisture content from a wet, solid material by converting some of this moisture into the gas state. The drying conditions applied, i.e. the gas velocity, the inlet gas temperature and humidity and the drying time, influence the quality of the dried product. In analyses of drying, convective transfer coefficients are important parameters for the prediction of drying rates and temperatures.

Experimental results were earlier reported concerning the coupling of heat and mass transfer phenomena around differently shaped materials under different conditions (SSU-HSueh and T.R. Marerro, 1996.; Szentgyörgyi et al., 2000). Following a considering of the transport coupling effects, experimental results relating to the loss of moisture and the surface temperature indicate various ways to calculate the heat transfer coefficients, using dimensionless numbers. The coupled heat and mass transfer results are correlated in terms of the dimensionless Nusselt and Sherwood numbers. The dried materials were porous and had simple shapes: plates and cylinders. (A. Kondjoyan, F. Péneau, H-C. Boisson, 2002.)

Free stream turbulence has been claimed to influence the heat transfer coefficients in the cases of plates, circular cylinders and elliptical cylinders (Kondjoyan and Daudin, 1995; Kondjoyan et al.,

2002). The transfer coefficient increases as a function of the free stream turbulence level either in the laminar boundary layer or in the turbulent boundary layer. (Kondjoyan and Daudin, 1993). Others found that the measured heat transfer coefficient is twice larger than the coefficient predicted for heat transfer only. (Szentgyörgyi et al., 2000; SSU-H.Sueh and T.R. Marerro, 1996.) as it can be seen in Figure 2 and 3.

The aim of our work was to confirm the existence of divergences at the heat transfer coefficients around single spheres during convective drying as well. Otherwise this paper suggests the reason of the divergence at Nusselt numbers and proves it by hydrodynamic and mathematical model in case of flat plate.

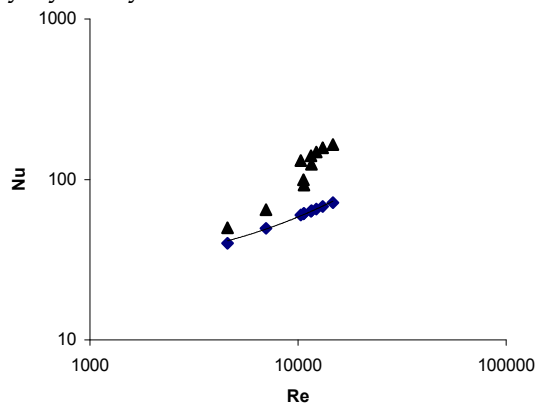


Figure 2. Nu numbers derived from experiment (▲) and calculated from literature (◆) for plates, (Szentgyörgyi et al., 2000)

## 2. MATERIAL AND METHODS

### 2.1. Apparatus and drying conditions

The experimental way used in this study adopted from (Kondjoyan and Daudin, 1993). A horizontal drying chamber was made for this study. The cross-section of the chamber was 0,1 m<sup>2</sup>. The chamber operated with a fan. The fan was placed in the inlet pipe, and this inlet pipe contained filaments to warm up the drying air. The air temperature was kept on a constant level at each experiment. The air velocity was controlled on a constant level. The experiments were repeated four or five times with the same sized plates (O. Molnár, 2004) and sphere on a different velocity level.

The drying material was placed onto a special frame in the area of free stream. The frame had tripod standing outside of the chamber on a balance. By this way, the weight loss of the sphere was under on-line control. The inlet air temperature, humidity and the pressure-drop were measured at the inlet pipe. The air temperature in the drying chamber and the inside temperature of the sphere were measured by a sensor and thermocouples. All parameters were registered in a computer.

### 2.2. Material

The materials used in our experiments were different size of spheres which diameter was 29 mm; 38 mm; 41 mm. These spheres were made of gypsum and gypsum mixed with paper. Three thermocouples were inserted into the spheres: into the middle, near the surface and one between these. The prepared spheres were put under water to hydration for eight hours before the experiments.

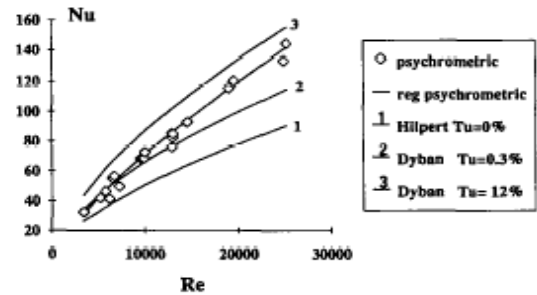


Figure 1. The effect of turbulence on heat transfer Nu at cylinder (A. Kondjoyan and J.D. Daudin, 1993)

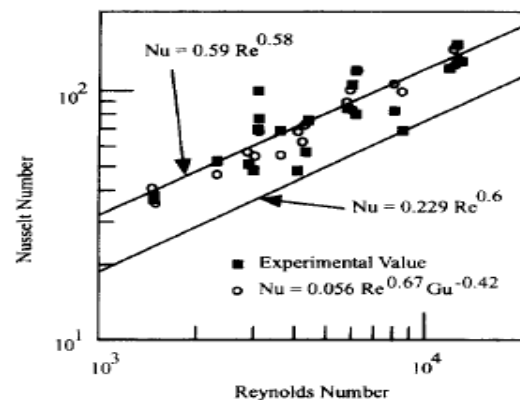


Figure 3. Nu numbers derived from experiment ( $Nu=0,59Re^{0,58}$ ) and calculated from literature ( $Nu=0,229Re^{0,6}$ ) and a corrected Nu for cylinder (SSU-HSueh and T.R. Marerro, 1996)

### 2.3. Theoretical analysis

The first part of this study pays attention on the constant rate period of convective drying around single spheres. During convective drying, simultaneous heat and mass transfer exist. The drying process consists of three main periods: the first is the 'developing' period; the second is the 'constant rate' period and the third one is the 'falling rate' period.

The constant rate period is well observable from the weight loss of the sphere. The weight of the wetted, gypsum sphere decreases consistently until 30 minutes, see figure 4, marked with  $\blacklozenge$ -line. As assumed before, the evaporation is characteristically for the constant rate period therefore the temperature of the material is constant. This shows well the  $\Delta \circ \diamond$ -marked lines on the Figure 4.

In this period, the surface of the material is supposed to be covered totally by water. Therefore, the surface temperature is equal to the wet bulb temperature at any point of the body. The wet bulb temperature depends on the air temperature and the humidity.

In coupling transport phenomena, the heat flux coming from the hot, ambient air turns into the phase change of the moisture content of the material and otherwise increases the temperature of the drying material. There are Nusselt numbers proposed by (F. P. Incropera and D.P. DeWitt, 1995) and (T. Környei, 1999) with which the heat transfers could be described around a single sphere.

$$Nu_{lit,1} = \left[ 2 + (0,4 \cdot Re^{1/2} + 0,06 \cdot Re^{2/3}) \cdot Pr^{0,4} \right] \cdot \left( \frac{\mu_G}{\mu_{sp}} \right)^{1/4} \quad (1)$$

A special case of convection heat transfer from spheres relates to the heat transport from freely falling drops. The equation is suggested in (F. P. Incropera and D.P. DeWitt, 1995).

$$Nu_{lit,2} = 2 + 0,6 \cdot Re^{0,5} \cdot Pr^{0,33} \quad (2)$$

These equations provided the basis for comparison with the experimental Nusselt numbers around our single spheres.

The second part of this study pays attention for the theoretical analysis based on mathematical approach of transport phenomenon around a flat plate. The circumstances of the flat plate experiments were the same as our single sphere experiment had.

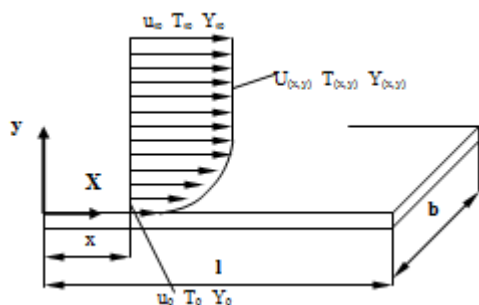


Figure 5. The velocity profile of the drying air over the flat plate

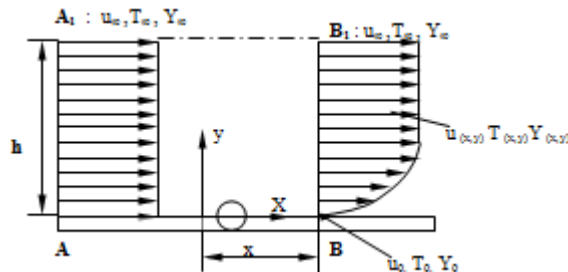


Figure 6. The theoretical control panel of the drying air

The surface of the flat plate is covered with liquid in the constant rate period of drying. We suppose that the air velocity is bigger than zero in the boundary layer at the surface. Our suggestion of this velocity condition is the existence of a skin friction occurred by the wet surface.

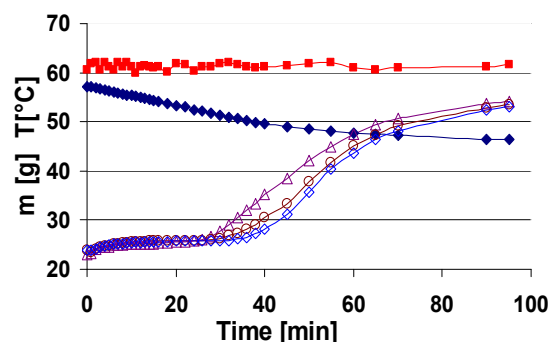


Figure 4. Drying parameters of the sphere (diameter 41 mm,  $\blacksquare$  air temperature 60°C; air velocity 2,39 ms<sup>-1</sup>):  $\blacklozenge$  m-weight loss;  $\Delta \circ \diamond$ : T<sub>s</sub>-inside temperature of the sphere

The Fig. 5 shows the boundary layer parameters over the flat plate. For the mathematical consideration were used a theoretical control panel to define impulse, energy- and mass balance equations as it shows Figure 6 and Figure 8. The Fig. 7 presents the skin friction on the surface influencing the heat transfer and the mass transfer.

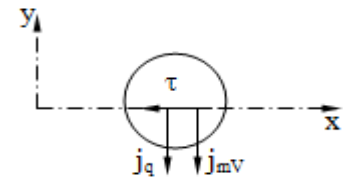


Figure 7.: the influence of the skin friction (regarding Fig. 6.)

Table 1.: Balance equations for the drying air

Cross section	Mass balance of the air	Impulse balance	Energy balance	Mass balance of the vapor
AA1	$-\rho b \int_0^h U_\infty dy$	$-\rho b \int_0^h U_\infty^2 dy$	$-\rho b c_p \int_0^h T_\infty U_\infty dy$	$-\rho b \int_0^h T_\infty U_\infty dy$
BB1	$-\rho b \int_0^h u dy$	$-\rho b \int_0^h u^2 dy$	$-\rho b c_p \int_0^h T u dy$	$-\rho b \int_0^h T u dy$
A1B1	$-\rho b \int_0^h (U_\infty - u) dy$	$-\rho b \int_0^h U_\infty (U_\infty - u) dy$	$-\rho b c_p \int_0^h T_\infty (U_\infty - u) dy$	$-\rho b \int_0^h Y_\infty (U_\infty - u) dy$
AB	0	$-b \int_0^x \tau_0 dx$	$b \int_0^x j_q dx$	$b \int_0^x j_{mV} dx$
$\sum_{y=0}^{y=h \rightarrow \infty}$	The mass amount of the inlet and outlet gas is =0	The resultant forces on the plate are=0	The resultant of the inlet energy streams are=0	The resultant of vapor mass transfers are=0

The impulse balance:

$$\rho b \int_0^\infty u(u - U_\infty) dy = b \int_0^x \tau_0 dx \quad (1a)$$

The energy balance:

$$\rho b c_p \int_0^\infty u(T - T_\infty) dy = b \int_0^x j_q dx \quad (1b)$$

The vapor mass balance

$$\rho b \int_0^\infty (Y - Y_\infty) dy = b \int_0^x j_{mV} dx \quad (1c)$$

Create the dimensionless distributions of the boundary layer conditions:

Dimensionless velocity:

$$\bar{u} = \frac{u - u_0}{U_\infty - u_0} = f_u(\eta_u) \quad (2a)$$

Dimensionless temperature:

$$\bar{T} = \frac{T - T_0}{T_\infty - T_0} = f_T(\eta_T) \quad (2b)$$

Dimensionless wet content of the vapor:

$$\bar{Y} = \frac{Y - Y_0}{Y_\infty - Y_0} = f_Y(\eta_Y) \quad (2c)$$

The  $U_\infty$ ;  $u_0$ ;  $T_\infty$ ;  $T_0$ ;  $Y_\infty$  and  $Y_0$  are constant and the boundary distributions depend only on the dimensionless thickness:

$$\eta_u = \frac{y}{\delta_u(x)}, \quad \eta_T = \frac{y}{\delta_T(x)}, \quad \eta_Y = \frac{y}{\delta_Y(x)} \quad (3a,b,c)$$

Writing the thickness of boundary layer as a polynomial approach (Welty, Wicks, Wilson, Rorrer, 2007.) (S. Szentgyörgyi, K. Molnár, M. Parti 1986.):

$$f(\eta) = a_0 + a_1\eta + a_2\eta^2 + a_3\eta^3 + a_4\eta^4 \quad (4)$$

Taking into consideration the conditions below:

$$\begin{aligned} \text{at } \eta=0: & \quad f(\eta)=0; \quad f''(\eta)=0 \quad \text{and} \\ \text{at } \eta \geq 1: & \quad f(\eta)=1, \quad f''(\eta)=0 \end{aligned} \quad (5)$$

The derivatives of the Eq. (4) are:

$$f'(\eta) = 2\eta - 2\eta^3 + \eta^4 \quad (6)$$

and

$$f'(\eta)_{\eta=0} = \beta = 2 \quad (7)$$

Using the Eq. 2a, the velocity profile is:

$$u = f_u(U_\infty - u_0) + u_0 \quad (8)$$

if x-parameter is constant we can write with Eq. (3a):

$$dy = \delta_u d\eta_u \quad (9)$$

where:

$$\begin{aligned} \text{at } y=0: & \quad \eta_u=0, \\ \text{at } y=\infty: & \quad \eta_u=1. \end{aligned}$$

Since Eq. (5) state at  $h>1$   $f_u=1$ , the integral (1a) extends only to 1. This establishment and Eq. (8) and (9) lead to:

$$\int_{y=0}^{\infty} u(U_\infty - u) dy = \int_{\eta=0}^1 [f_u(U_\infty - u_0) + u_0] \{U_\infty - [f_u(U_\infty - u_0) + u_0]\} \delta_u d\eta_u \quad (10)$$

Reducing Eq (10) we have that:

$$\int_{y=0}^{\infty} u(U_\infty - u) dy = \delta_u(x) [(U_\infty - u_0)^2 \int_0^1 f_u(1 - f_u) d\eta_u + u_0(U_\infty - u_0) \int_0^1 (1 - f_u) d\eta_u] \quad (11)$$

Define the integrals in Eq. (11) as follows:

$$\alpha_1 = \int_0^1 f_u(1 - f_u) d\eta_u \quad (12)$$

and

$$\alpha_2 = \int_0^1 (1 - f_u) d\eta_u \quad (13)$$

We can state that  $\alpha_1=37/315$  and  $\alpha_2=3/10$  are only constant numbers refer to (Welty, Wicks, Wilson, Rorrer, 2007.) since  $f_u$  depends on  $\eta_u$  only in Eq. (6). Using our statement and Eq (1a), (12), (13), the Eq. (11) turns to:

$$-\frac{\tau_0}{\rho} = \frac{d}{dx} \int_{y=0}^{\infty} u(U_\infty - u) dy = \frac{d\delta_u}{dx} [(U_\infty - u_0)^2 \cdot \alpha_1 + u_0(U_\infty - u_0) \cdot \alpha_2] \quad (14)$$

Define  $\tau_s$  as the skin friction on the surface we can write the force as well.  $\tau_0$  has the same value, but negative since it belongs to the ambient air.

$$\tau_s = \mu \cdot \left( \frac{\partial u}{\partial y} \right)_{y=0} = -\tau_0 \quad (15)$$

Assembling the Eq. (15), (2a)(3a):

$$-\frac{\tau_0}{\rho} = \nu \left( \frac{\partial u}{\partial y} \right)_{y=0} = \nu(U_\infty - u_0) \left( \frac{df_u}{d\eta_u} \right)_{\eta_u=0} \cdot \frac{d\eta_u}{dy} = \nu(U_\infty - u_0) \cdot f'_u(0) \cdot \frac{1}{\delta_u} \quad (16)$$

Combine the Eq. (16) with Eq. (7) and (14) we have:

$$\beta_u \cdot \frac{v(U_\infty - u_o)}{\delta_u} = [(U_\infty - u_o)^2 \cdot \alpha_1 + u_o \cdot (U_\infty - u_o) \cdot \alpha_2] \cdot \frac{d\delta_u}{dx}$$

Reducing the equation written below we can state that:

$$\delta_u \frac{d\delta_u}{dx} = \frac{\beta_u v}{(U_\infty - u_o)\alpha_1 + u_o\alpha_2} = \text{const} \tan s \quad (17)$$

Since Eq (17) is constant, it can be integral after separation:

$$\int_0^{\delta_u} \delta_u d\delta_u = \frac{\delta_u^2}{2} = \int_0^x \frac{\beta_u v \cdot dx}{(U_\infty - u_o)\alpha_1 + u_o\alpha_2} = \frac{\beta_u v}{(U_\infty - u_o)\alpha_1 + u_o\alpha_2} \cdot x$$

After determine the integral of Eq. (17), Eq. (18) delivers the momentum equation of boundary layer

$$\delta_u = \sqrt{\frac{\beta_u v \cdot x}{(U_\infty - u_o)\alpha_1 + u_o\alpha_2}} \quad (18)$$

When  $u_o=0$ , we can reduce Eq. (18) further:

$$\delta_u \Rightarrow \delta_u^* = \sqrt{\frac{\beta_u v \cdot x}{\alpha_1 U_\infty}} \quad (19)$$

Create the  $\delta_u / \delta_u^*$  :

$$\frac{\delta_u^*}{\delta_u} = \sqrt{\frac{(U_\infty - u_o)\alpha_1 + u_o\alpha_2}{U_\infty\alpha_1}} = \sqrt{1 - \frac{u_o}{U_\infty} + \frac{\alpha_2 u_o}{\alpha_1 U_\infty}} \quad (20)$$

and define K and P as follows:

$$\frac{\alpha_2}{\alpha_1} := K \quad \text{and} \quad \frac{u_o}{U_\infty} := P \quad (21) (22)$$

K is 2,554 referring to Eq. (12)(13)

Taking into consideration the Eq. (21)(22) at Eq (20) and express the  $\delta_u$  , we get to the following:

$$\frac{\delta_u^*}{\delta_u} = \sqrt{1 + (K - 1)P}$$

$$\delta_u = \delta_u^*(x) \frac{1}{\sqrt{1 + (K - 1)P}} \quad (23)$$

where  $\delta_u = \delta_u(x, P)$  and using the constant value of K:

$$\delta_u = \delta_u^*(x) \frac{1}{\sqrt{1 + (2,554 - 1)P}} \quad (24)$$

Studying Eq.(24) we can establish that:

- ✓ Since  $P \geq 0$ , therefore  $\delta_u \leq \delta_u^*$ ,
- ✓ it follows from the foregoing that the boundary layer on the surface is thinner when the velocity is  $u_o > 0$ .
- ✓ This phenomenon increases the value of  $|\tau_o|$ .

If we put Eq.(24) into Eq (16) :

$$-\frac{\tau_o}{\rho} = v(U_\infty - u_o)\beta_u \frac{1}{\delta_u} = v(U_\infty - u_o)\beta_u \frac{\sqrt{1 + (K - 1)P}}{\delta_u^*}, \quad (25)$$

Explaining Eq. (25), the value of  $|\tau_o|$  is decreasing if there is  $(U_\infty - u_o)$  instead of  $U_\infty$  on the right side of the Eq.(25).

Taking  $u_o=0$ , than P is zero and Eq (25) turns to:

$$\left(-\frac{\tau_o}{\rho}\right) \Rightarrow \left(-\frac{\tau_o}{\rho}\right)^* \equiv \frac{vU_\infty\beta_u}{\delta_u^*} \quad (26)$$

Define the quotient of Eq (25) and (26) with Eq. (22, 23), it results Eq. (27).

$$\frac{\overline{\tau_0}}{\tau_0} = \frac{\tau_0}{\tau_0^*} = (1-P)\sqrt{1+(K-1)P} = \sqrt{(1-P)^3 + KP(1-P)^2} \quad (27)$$

### 3. RESULTS AND DISCUSSION

Taking the measurements into consideration we observed similar phenomenon as other done in case of flat plate and cylinders during the steady state period of convective drying. The calculated Nusselt numbers are significantly higher than the Nusselt numbers derived from the equations predicted the literature and determined in Eq. (1)(2) in case of single sphere; as it show Fig (8) (9).

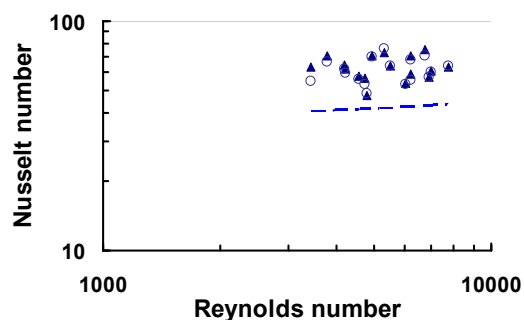


Figure 8. Nusselt numbers as a function of Reynolds number for single spheres in drying:  $\circ$   $\blacktriangle$ - experimental values dashed line means  $Nu_{lit,1}$  derived from Eq. (1).

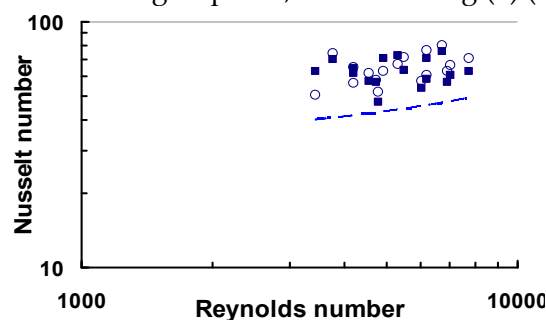


Figure 9. Nusselt numbers as a function of Reynolds number for sphere-like drops:  $\circ$   $\blacktriangle$ -experimental values dashed line means  $Nu_{lit,2}$  derived from Eq. (2)

On the basis of the mathematical approach we can state that the momentum transfer is influenced by the skin friction we suggested. Observing the Eq. (27) we can state that the value of  $|\tau_0|$  is smaller than 1 at  $P>0$ . The function has a tendency of monotonously decrease in the interval of  $0 \leq \tau_0$

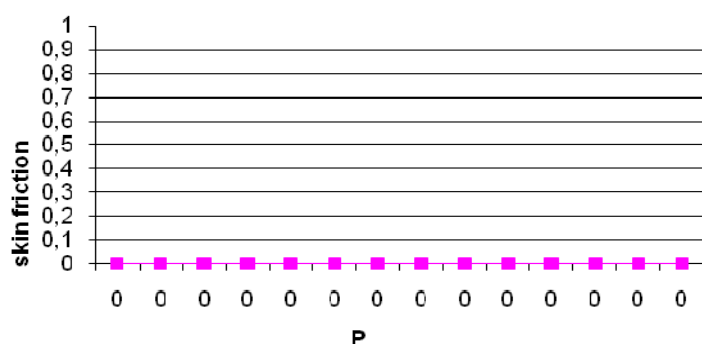


Figure 10. The  $\tau_0$  skin friction vs  $P = u_0/U_\infty$  (relative air velocity)

The reason is proved by next conditions: the  $\tau_0=1$  at  $P=0$  and  $\tau_0=0$  at  $P=1$ . The tendency of the function shows Fig. 10.

The Eq. (27) and the Figure 10 prove that the value of the  $\tau_0$  skin friction causes hydrodynamic force on the drying surface decreases by increasing the  $u_0$  velocity.

#### NOMENCLATURE

$U, u:$	velocity [m/s]
$T:$	temperature [K]
$Y$	absolute moisture content of the air [kg kg <sup>-1</sup> ]
$K, P$	defined in Eq. (21, 22)
$c_p$	specific heat of the air [Jkg <sup>-1</sup> K <sup>-1</sup> ]
$h$	heat transfer coefficient [W m <sup>-2</sup> K <sup>-1</sup> ]
$j_q$	heat flux [W m <sup>-2</sup> ]
$j_m V$	mass flux [kg m <sup>-2</sup> s <sup>-1</sup> ]
$f_u, f_r, f_Y$	: dimensionless form of boundary layer conditions
$A, A1, B, B1:$	basis of the control panel
$l, b:$	length and width of the plate
$x, y$	coordinates
$v$	air velocity [m s <sup>-1</sup> ]

#### Greek symbols

$\alpha$	defined in Eq. (12,13)
$\beta$	defined in Eq. (7)
$\lambda$	thermal conductivity [Wm <sup>-1</sup> K <sup>-1</sup> ]
$\mu$	dynamic viscosity [Pas]
$\eta (u, T, Y):$	dimensionless thicknesses
$\rho$	density [kg m <sup>-3</sup> ]
$\nu$	kinematical viscosity [m <sup>2</sup> s <sup>-1</sup> ]
$\tau$	skin friction
$\delta_u, \delta_T, \delta_Y$	: the thickness of momentum-, heat-, moisture boundary layers in the air

**Subscripts**

0	surface condition
$\infty$	main stream condition of the air
G	gas, air condition
u	refer to velocity
T	refer to temperature
Y	refer to vapour content of the air

sp	sphere condition
lit	taken from the literature
wb	wet bulb condition

**Dimensionless groups**

Nusselt number	$hD_{sp}/\lambda$
Reynolds number	$vD_{sp}/\nu$
Prandtl number	$\nu/a$

**REFERENCES**

- [1.] Kondjoyan, F. Péneau, H-C. Boisson, 2002.: Effect of high free stream turbulence on heat transfer between plates and air flows (Review). Int. J. Therm. Sci. Vol 41. pp. 1-6.
- [2.] Kondjoyan, J.D. Daudin, 1993: Determination of transfer coefficients by psychrometry. Int. J. Heat Mass Transfer Vol. 36. (7) pp. 1807-1818.
- [3.] Kondjoyan, J.D. Daudin, 1995: Effects of free stream turbulence intensity on heat and mass transfer at the surface of circular and an elliptical cylinder, axis ratio 4. Int. J. Heat Mass Transfer vol. 38. (10) pp. 1735-1749.
- [4.] Frank P Inncoropera, David P De Witt 1985. Fundamentals of heat and mass transfer. John Wiley & Sons Inc., New York, pp. 339-340.
- [5.] James R. Welty, Charles E. Wicks, Robert E. Wilson, Gregory L. Rorrer 2007.: Fundamentals of Momentum, Heat, and Mass Transfer, John Wiley & Sons, Inc. Oregon
- [6.] O. Molnár 2004. Behúzódó párolgási front és a hőátadási tényező szárításkor. Doktori értekezés. Budapesti Műszaki és Gazdaságtudományi Egyetem.
- [7.] S. Szentgyörgyi, K. Molnár, M. Parti 1986. Transzportfolyamatok Tankönyvkiadó, Budapest, pp. 343.
- [8.] S. Szentgyörgyi, L. Tömösy, O. Molnár, (2000): Convection Heat Transfer Coefficients at Convective Drying of Porous Materials, Drying Technology 18(6), 1287-1304.
- [9.] SSU-Hsueh Sun, Thomas R. Marrero 1996: Experimental study of simultaneous heat and mass transfer around single short porous cylinders during convection drying by a psychrometry method. Int. J. Heat Mass Transfer, Vol. 39 (17), pp. 3559-3565.
- [10.] T. Környei, 1999., Hőátvitel, Műegyetemi Kiadó. pp. V-10



ANNALS of Faculty Engineering Hunedoara – International Journal of Engineering



copyright © UNIVERSITY POLITEHNICA TIMISOARA, FACULTY OF ENGINEERING HUNEDOARA,  
5, REVOLUTIEI, 331128, HUNEDOARA, ROMANIA  
<http://annals.fih.upt.ro>